Contrib Mineral Petrol (1990) 105:381–392

Contributions to Mineralogy and Petrology

Nd- and Sr-isotopic compositions of lavas from the northern Mariana and southern Volcano arcs: implications for the origin of island arc melts

P.N. Lin[1,*], R.J. Stern[1], J. Morris[2], and S.H. Bloomer[3]

[1] Center for Lithospheric Studies, University of Texas at Dallas, Box 830688, Richardson, TX 75083-0688, USA
[2] Department of Terrestrial Magnetism, Carnegie Institution of Washington, 5241 Broad Branch Road, NW, Washington, DC 20015, USA
[3] Department of Geology, Boston University, 675 Commonwealth Avenue, Boston, MA 02215, USA

Abstract. Nd- and Sr-isotopic data are reported for lavas from 23 submarine and 3 subaerial volcanoes in the northern Mariana and southern Volcano arcs. Values of ε_{Nd} range from +2.4 to +9.5 whereas $^{87}Sr/^{86}Sr$ ranges from 0.70319 to 0.70392; these vary systematically between and sometimes within arc segments. The Nd- and Sr-isotopic compositions fall in the field of ocean island basalt (OIB) and extend along the mantle array. Lavas from the Volcano arc, Mariana Central Island Province and the southern part of the Northern Seamount Province have $\varepsilon_{Nd} = +4$ to +10 and $^{87}Sr/^{86}Sr =$ 0.7032 to 0.7039. These are often slightly displaced toward higher $^{87}Sr/^{86}Sr$ at similar ε_{Nd}. In contrast, those lavas from the northern part of the Mariana Northern Seamount Province as far north as Iwo Jima show OIB isotopic characteristics, with $\varepsilon_{Nd} < +5$ and $^{87}Sr/^{86}Sr =$ 0.7035 to 0.7039. Plots of $^{87}Sr/^{86}Sr$ and ε_{Nd} versus Ba/La and $(La/Yb)_n$ support a model in which melts from the Mariana and Volcano arcs are derived by mixing of OIB-type mantle (or melts therefrom) and a metasomatized MORB-type mantle (or melts therefrom). An alternate interpretation is that anomalous trends on the plots of Nd- and Sr-isotopic composition versus incompatible-element ratios, found in some S-NSP lavas, suggest that the addition of a sedimentary component may be locally superimposed on the two-component mixing of mantle end-members.

Introduction

Isotopic studies of ocean-island and ocean-ridge basalts have stressed the heterogeneity of the upper mantle and demonstrated the various scales of these heterogeneities. Concepts of the different scales of upper mantle heterogeneity have been applied to the origin of arc magmas and particularly those from intra-oceanic island arcs (Morris and Hart 1983; White and Patchett 1984; Ewart and Hawkesworth 1987). Lavas from these areas have the advantage of being erupted through oceanic crust, precluding contamination by continental crust, therefore simplifying the interpretation of geochemical and isotopic data.

However, there is still disagreement concerning the sources which contribute to arc magmas. Consequently, the research foci include the degree of sediment incorporated into the source of arc melts (Armstrong 1971; McLennan and Taylor 1981; White and Dupre 1986), the effects of crystal fractionation (Stern 1979; Woodhead 1988), and source metasomatism and/or mixing (Arculus and Powell 1986; Vargas and Reagan 1987; Ellam and Hawkesworth 1988). Many workers favor multi-stage petrogenetic models which can account for the great range of chemical and isotopic characteristics of arc lavas (Arculus and Johnson 1978; Perfit et al. 1980). Metasomatism of mantle peridotite by fluids derived from subducted lithosphere has been argued for some arcs, such as the Aleutians (McCulloch and Perfit 1981) and supported by the results of high-pressure experiments (Tatsumi et al. 1986). The plum-pudding or blob model of heterogeneity deduced for the oceanic mantle (Batiza 1984; Davies 1984; Zindler et al. 1984) has been applied to arcs as well (Morris and Hart 1983; Gill 1984). Unfortunately, mixtures of these different components from the mantle wedge are not readily distinguished from subduction-related components, such as the metasomatic fluids from the subducted slab or pelagic sediment. The multiplicity of potential sources greatly complicates reconstructing arc petrogenesis.

In this paper, we contribute to the resolution of this problem by presenting new Nd- and Sr-isotopic data for lavas from the northern Mariana arc and southern Volcano arc. These data show significant variation in the isotopic compositions of the lavas, in a geographically regular manner. These data, in addition to related trace element data (Lin et al. 1989), lead to well-con-

* Now at: Byrd Polar Research Center, Ohio State University, 125 S. Oval Mall, Columbus, OH 43210, USA

Offprint requests to: P.N. Lin

strained mixing models to explain the origin of melts for this arc system. The geographic variation permits speculation on the links between chemistry and tectonic setting.

Geological setting and previous work

The Mariana Island arc lies in the western Pacific. Following the geographic distribution of volcanic islands and seamounts, the Mariana arc has been subdivided into three provinces (Stern et al. 1988; Bloomer et al. 1989a): the Southern Seamount Province (SSP, Lat. 13°N–16°N), the Central Island Province (CIP, Lat. 16°N–20.7°N), and the Northern Seamount Province (NSP, Lat. 20.7°N–24°N; Fig. 1). The NSP is further divided into southern and northern segments (S-NSP, Lat. 20.7°–23.1°N and N-NSP, 23.4°–24°N) due to the distinctive large ion lithophile (LIL) and

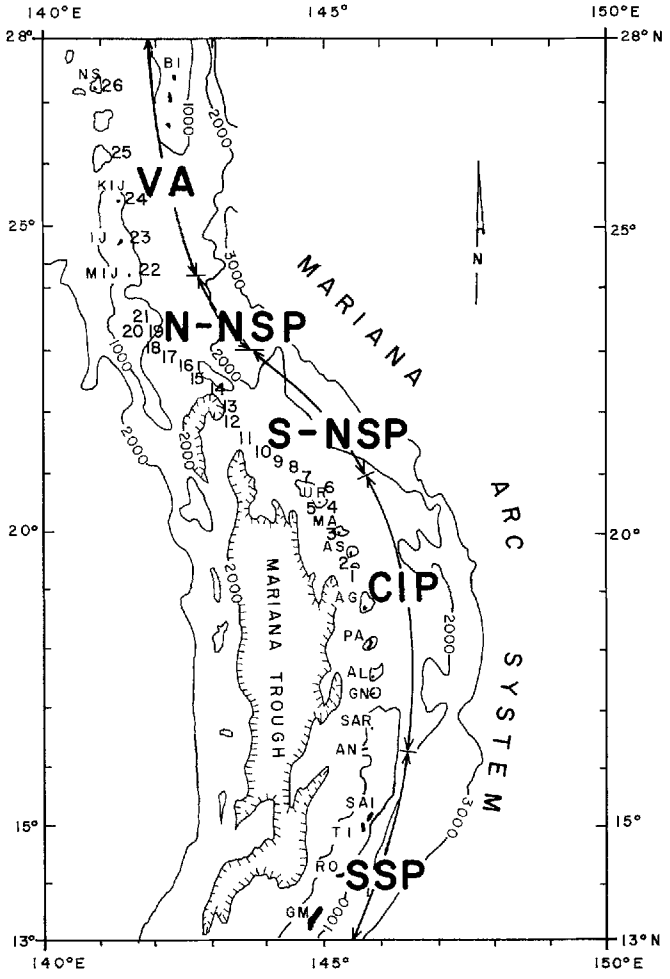

Fig. 1. Location map for the Mariana arc and Volcano arc (modified from Chase et al. 1968). Contour intervals are in fathoms (1 fathom = 1.829 m). Location of major islands are also shown: *GM*, Guam, *RO*, Rota, *TI*, Tinian, *SAI*, Saipan, *AN*, Anatahan, *SAR*, Sarigan, *GN*, Guguan, *AL*, Alamagan, *PA*, Pagan, *AG*, Agrigan, *AS*, Asuncion, *MA*, Maug, *UR*, Uracas, *MIJ*, Minami Iwo Jima, *IJ*, Iwo Jima, *KIJ*, Kita Iwo Jima, *NS*, Nishino Shima, *BI*, Bonin Islands. *Bold labels* are: *VA*, Volcano Arc, *N-NSP*, Northern part of Northern Seamount Province, *S-NSP*, Southern part of Northern Seamount Province, *CIP*, Central Island Province, *SSP*, Southern Seamount Province. *Numbers* indicate sample location of seamounts and volcanoes which are included in this study and identified in Table 1

light rare earth element (LREE) enrichments observed for the N-NSP (Stern et al. 1988). The volcanoes from Minami Iwo Jima (24°N) to Nishino-Shima (27°N) belong to the Volcano arc (VA), sometimes referred to as the Bonin Arc (Honza and Tamaki 1985). Because Iwo Jima shares the distinctive enrichments of the N-NSP, it is included here as part of the N-NSP in spite of the fact that geographically it belongs to the Volcano arc.

Previous investigations of lavas from the Mariana arc concentrated on the islands (Meijer 1976; DePaolo and Wasserburg 1977; Stern 1979; Dixon and Batiza 1979; White and Patchett 1984; Hole et al. 1984; Woodhead and Fraser 1985; Ito and Stern 1986; Woodhead et al. 1987; Woodhead 1988). Studies of the subaerial edifices have led to a consensus: that CIP lavas are dominated by fractionated basalts having chemical characteristics intermediate between low-K arc tholeiites and low-K calc-alkaline suites, with minor andesites resulting from low-P fractional crystallization involving anhydrous phases (Stern 1979; Dixon and Batiza 1979; Meijer and Reagan 1981; Woodhead 1988). There is a general recognition that the isotopic- and incompatible-element ratios show remarkably little variation from volcano to volcano (Chow et al. 1980; Dixon and Batiza 1979; Stern 1981, 1982; Stern and Ito 1983), but controversy persists regarding the sources involved in magma generation. This argument concerns the relative roles played by the subducted lithosphere and sediment (Kay 1980; White and Patchett 1984; Hole et al. 1984; Woodhead and Fraser 1985) as opposed to that of the mantle wedge (DePaolo and Wasserburg 1977; Stern 1981; Stern and Ito 1983; Ito and Stern 1986).

Studies have recently been extended to include submarine volcanoes (Garcia et al. 1979; Wood et al. 1981; Dixon and Stern 1983; Stern and Bibee 1984; Lin et al. 1986; Jackson and Fryer 1988). The results of recent efforts to sample all of the submarine volcanoes along the magmatic front of the arc have led to some surprises. Lavas from the SSP and NSP show greater compositional variability than that seen in the CIP, including variation in mineralogy, major and trace element chemistry, and isotopic compositions. Lavas from the SSP are as evolved as those from the larger CIP edifices (Dixon and Stern 1983; Stern and Bibee 1984). In contrast to the predominantly basaltic CIP, S-NSP edifices contain abundant hornblende andesites and more felsic lavas, with modest enrichments in LIL and LREE (Bloomer et al. 1989b). Lavas from the N-NSP are approximately saturated in silica, contain atypical phenocryst assemblages (including biotite in some cases), and have strong enrichments in LIL and LREE (Stern et al. 1988; Bloomer et al. 1989b). The strong enrichments observed in N-NSP lavas, however, are accompanied by lower values of certain elemental ratios typically thought to be diagnostic of arc lavas (i.e., Ba/La and Sr/Nd; Lin et al. 1989). The incompatible element data have led to the development of a two-component mixing model for the Mariana arc as shown on Fig. 2 (Lin et al. 1989). In this paper, we evaluate and modify this model using Nd- and Sr-isotopic data.

Analytical procedures

The samples picked for isotopic analyses were chosen from those previously analyzed for LIL and rare earth elements (REE) (Lin et al. 1989). All samples were slabbed and then cleaned by consecutively boiling in de-ionized water, rinsing in acetone, re-boiling in de-ionized water, and ultrasonification in distilled water. The chemical procedures for Sr-isotope determinations have been described elsewhere (Stern and Bibee 1984). A procedure modified after that of Richard et al. (1976) was adopted to separate Nd from Sm for the measurement of Nd-isotopic compositions. Strontium- and neodymium-isotopic compositions (Table 1) were measured on unleached samples. Subsequently, some samples were leached with 2.5 N HCl for 4 hours and four samples (D33-3-1, D38-2, D41-52, D77-1) with 6 N HCl for 18 hours. The determination of $^{87}Sr/^{86}Sr$ on most unleached samples was done on the 6 inch radius mass-spectrometer at UTD. Twenty-six analyses of the E+A $SrCO_3$ standard during the course of this study yielded a mean $^{87}Sr/^{86}Sr$ of 0.70810 ± 0.00010 (2σ). All leached samples

Table 1. Sr- and Nd- isotopic composition of igneous rocks from the Mariana and Volcano arcs

Sample	$^{87}Sr/^{86}Sr$		$^{143}Nd/^{144}Nd$	ε_{Nd}
	Unleached	Leached		
Central Island Province (CIP)				
1 Poyo Seamount (E)				
D8-1	0.70347±4[a]	–	–	–
D8-3	0.70357±7	–	–	–
2 Cheref Seamount (E)				
D9-6	0.70341±6	–	–	–
D9-7	0.70342±7	–	0.513065±17	+7.8
D9-20	0.70325±5	–	–	–
D10-1-2	0.70333±6	–	–	–
D10-2-6	0.70326±5	–	–	–
D10-2-7	0.70323±5	–	–	–
D10-2-11	0.70334±5	–	–	–
D11-11	0.70340±6	–	–	–
3 Supply Reef (D)				
D13-2	0.70329±6	–	0.513072±10	+7.9
D13-11	0.70335±6	–	–	–
D14-1	0.70330±5	–	–	–
D14-15	0.70350±5	–	–	–
4 Ahyi Seamount (A)				
D15-3-2	0.70336±4[a]	–	–	–
D15-3-3	0.70338±6	–	–	–
D16-3	0.70319±7	–	–	–
5 Makhahnas Seamount (D)				
D18-9	0.70340±4[a]	–	–	–
D18-11	0.70329±6	–	0.512990±11	+6.3
6 Uracas (A)				
UR-23	0.70354±5	–	–	–
7 NW Uracas Seamount (E)				
D19-3-5	0.70334±6	0.70338±4[a]	–	–
D19-3-10	0.70345±5	0.70342±4[a]	0.513062±34	+7.7
Southern-Northern Seamount Province (S-NSP)				
8 Chamorro Seamount (E)				
D23-3[b]	0.70352±6	0.70352±4[a]	–	–
9 S. Daikoku Seamount (D)				
D25-1[b]	0.70350±5	0.70349±4[a]	0.512986±11	+6.3
D25-8[b]	0.70342±5	0.70348±4[a]	–	–
D25-18[b]	0.70355±6	0.70352±4	–	–
D26-3-1[b]	0.70353±6	0.70346±4	–	–
D26-4-5[b]	0.70346±6	0.70345±4	–	–
D26-4-6[b]	0.70343±6	0.70343±4	–	–
10 Daikoku Seamount (D)				
D29-1-1	0.70359±6	–	–	–
D29-1-2	0.70359±6	–	–	–
D29-2-2	0.70355±6	–	0.512935±9	+5.3
D29-2-3	0.70356±6	–	–	–
11 Eifuku Seamount (D)				
D30-6	0.70349±6	–	–	–
D30-7	0.70370±6	–	0.512867±14	+3.9
D30-8	0.70363±6	–	–	–
D31-1-4	0.70351±7	–	0.512895±8	+4.5
D31-1-6	0.70352±4	–	–	–
D31-2-2	0.70348±5	–	–	–
12 Kasuga Seamount (E)				
D33-3-1[b]	0.70375±7	(0.70365±4[a])	0.512996±16	+6.5
13 Fukujin Seamount (A)				
D34-1-2	0.70374±5	–	–	–
D34-2-2	0.70379±7	0.70381±4[a]	0.512884±15[a]	+4.3
D35-1-2	0.70384±5	0.70378±4[a]	0.512903±17	+4.6
D35-2-1	0.70375±10	0.70374±4[a]	0.512926±15[a]	+5.1
14 Fukuyama Seamount (E)				
D38-2[b]	0.70405±7	0.70392±4[a] (0.70384±4[a])	0.512977±10	+6.1
15 Soyo Seamount (E)				
D41-52[b]	0.70391±5	0.70383±4[a] (0.70379±4[a])	0.513003±20	+6.6
16 Ichiyo Seamount (E)				
D44-1-5	0.70389±7	0.70385±4[a]	0.512904±10	+4.7
17 Nikko Seamount (A)				
D45-11	0.70369±6	–	0.512926±11	+5.1
D46-1-1	0.70370±4	–	0.512922±13	+5.0
Nothern-Northern Seamount Province (N-NSP)				
18 Ko-Hiyoshi Seamount (D)				
D47-1-1	0.70392±6	0.70385±4[a]	0.512782±15[a]	+2.3
19 S. Hiyoshi Seamount (A)				
D48-1-2	0.70379±6	–	0.512844±7	+3.5
D49-PB	0.70358±6	–	0.512848±9	+3.6
D49-1-2	0.70386±4	–	–	–
D49-2-1	0.70369±5	–	–	–
D49-3-2	0.70378±4[a]	–	–	–
20 Central Hiyoshi Seamount (D)				
D51-3	0.70371±6	–	0.512860±13	+3.8
D51-g(a)	0.70359±6	–	–	–
D51-g(b)	0.70350±7	–	0.512922±15	+5.0
D52-1-1	0.70383±5	–	0.512786±7	+2.4
D52-3-1	0.70374±17	–	0.512813±13	+2.9
21 N. Hiyoshi Seamount (D)				
D53-1-2	0.70387±5	–	0.512799±9	+2.6
D53-1-3	0.70385±5	–	0.512814±17	+2.9
D54-1-1	0.70383±5	–	–	–
22 Fukutoku Seamount (E)				
D55-1-2	0.70392±6	0.70393±4[a]	0.512795±14	+2.5
D57-6	0.70387±5	–	0.512821±17	+3.0
Volcano Arc (VA)				
23 Iwo Jima (A)				
IJ-trachy-andesite	0.70365±6	–	–	–
IJ-5-2	0.70375±8	–	0.512904±10	+4.7
IJ-7-2	0.70387±9	–	0.512913±10	+4.8
IJ-suribachi	0.70368±4	–	0.512914±9	±4.9
24 S. Kito Iwo Jima (E)				
D73-4-2	0.70355±7	–	–	–
D73-4-4	0.70362±6	–	–	–
25 Kaitoku (A)				
D75-4	0.70359±5	–	–	–
D77-1	0.70360±6	(0.70353±4[a])	0.513065±8	+7.8
26 Nishino Shima (A)				
D79-1	0.70344±4[a]	–	0.513150±22	+9.5
D79-6	0.70333±4[a]	–	–	–
D80-1	0.70347±4[a]	–	–	–
1973/74 Flow	0.70320±5[a]	–	0.513070±11	+7.9

(1) Values for ε_{Nd} are calculated using $\varepsilon_{Nd}=0$ for BCR-1 and $(^{143}Nd/^{144}Nd)_{BCR\text{-}1}=0.512665$

(2) Value of Sr isotopic composition for leached sample, without parentheses, was treated with 2.5N HCl 4 hours while those in parentheses were treated with 6N HCl 18 hours

(3) [a] Analyzed using Finnigan MAT 261 mass-spectrometer at UTD

(4) Codes in parentheses correspond to state of activity of volcano: *A*, active; *D*, dormant; *E*, extinct

(5) [b] Indicating Type II S-NSP lavas; all other S-NSP lavas are Type I

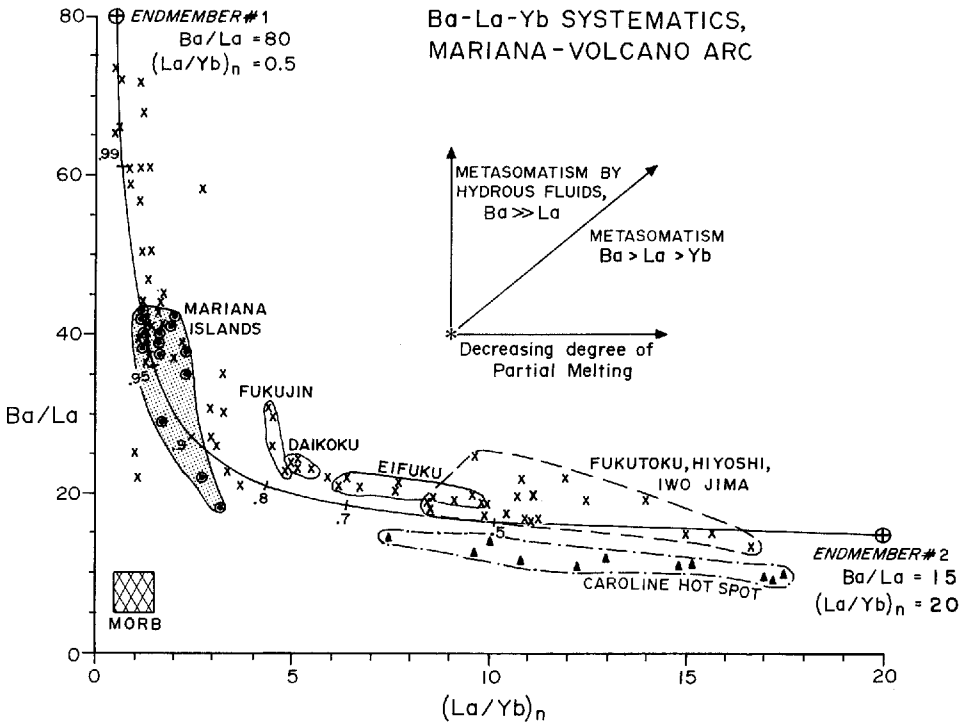

Fig. 2. Plot of Ba/La vs $(La/Yb)_n$ for samples from the Mariana-Volcano arc after Lin et al. (1989) to show the two-components mixing model. Samples from a western Pacific hot spot chain, Ponape in the Carolina Islands, are also shown (Dixon et al. 1984). Metasomatism by a fluid with an exceedingly high Ba/La and Ba/Yb would move source compositions vertically, while metasomatism involving a fluid where Ba > La > Yb would move compositions to the upper right; decreasing degrees of partial melting would move melt compositions horizontally to the right. None of these processes can acount for the hyperbolic trend which is best matched by mixing between two end-members. *Numbers* on the mixing curve are the fraction of Endmember #1

and some unleached samples were analyzed for Sr in the static mode on a newly installed Finnigan MAT 261 at UTD. Thirty one analyses of E+A $SrCO_3$ during the course of this study yielded a mean $^{87}Sr/^{86}Sr$ of 0.70805 ± 0.00004 (total range) on the Finnigan MAT 261. All Sr data is fractionation-corrected to $^{86}Sr/^{88}Sr = 0.11940$, and normalized to $^{87}Sr/^{86}Sr = 0.70800$ for E+A $SrCO_3$. Nd isotopic compositions were determined at DTM using the VG 354 multi-collector mass spectrometer and the 38 cm radius, 60° sector single-collector mass spectrometer. On the VG 354, Nd^+ signals were measured dynamically following the technique described in Walker et al. (1989). The current mean for 30 measurements of the La Jolla Nd standard is $^{143}Nd/^{144}Nd = 0.511865 \pm 0.000018$ (2σ). Nd isotope was analyzed as NdO^+ on the DTM 38 cm mass spectrometer and corrected for the oxygen-isotope composition reported by Nier (1950). Three samples were run at UTD on the MAT 261 using procedures outlined by Stern et al. (1990). $^{143}Nd/^{144}Nd$ ratios are normalized to $^{146}Nd/^{144}Nd = 0.72190$. The mean for 22 measurements of the La Jolla Nd standard is $^{143}Nd/^{144}Nd = 0.511857 \pm 0.000021$. Total processing blanks for Sr and Nd are 2 ng and 0.5 ng, respectively.

Results

The isotopic compositions of selected lavas from the northern Mariana and southern Volcano arcs are reported in Table 1. Samples are from active (A), dormant (D) and extinct (E) volcanoes, following the classification in Bloomer et al (1989a). For most samples, there is no significant difference between $^{87}Sr/^{86}Sr$ determined for leached and unleached samples. In three instances, samples from extinct volcanoes (D33-3-1, D38-2, D41-52) show significant lowering of $^{87}Sr/^{86}Sr$ (ca. 0.0002) following 6N HCl leaching. The range of Nd isotopic compositions is $\varepsilon_{Nd} = +2.4$ to $+9.5$. The geographic variation in isotopic compositions along the arc is shown on Fig. 3. There is a progressive decrease in ε_{Nd} along the arc from south (CIP, mean $\varepsilon_{Nd} = +7.0$) to north (S-NSP, mean $\varepsilon_{Nd} = +5.3$), where ε_{Nd} reaches a minimum (mean $\varepsilon_{Nd} = +3.6$) at N-NSP and Iwo Jima. Values increase again in the VA north of Iwo Jima (mean $\varepsilon_{Nd} = +8.4$). The mean Sr-isotopic composition increases in a complementary fashion from south (CIP, mean $^{87}Sr/^{86}Sr = 0.70343$) to north (S-NSP, mean $^{87}Sr/^{86}Sr = 0.70362$), reaching a maximum in the N-NSP and Iwo Jima (mean $^{87}Sr/^{86}Sr = 0.70376$), except some samples from S-NSP (e.g., Kasuga seamount, D33-3-1; Fukuyama seamount, D38-2; Soyo seamount, D41-52) which are possibly affected by seawater alteration and are explained in the following text. $^{87}Sr/^{86}Sr$ decreases again in the VA (mean $^{87}Sr/^{86}Sr = 0.70348$).

The Nd- and Sr-isotopic data for the Mariana and Volcano arc samples fall mostly within the mantle array, as previously noted (Fig. 4A; DePaolo and Wasserburg 1977; Stern 1981; Dixon and Stern 1983; White and Patchett 1984; Stern and Bibee 1984; Woodhead 1989). The new data extend considerably the known isotopic variability from the Mariana arc and show a range that is similar to that of the Hawaiian islands. In detail, the different geographic provinces have distinct isotopic characteristics (Fig. 4B). The field of Volcano arc sam-

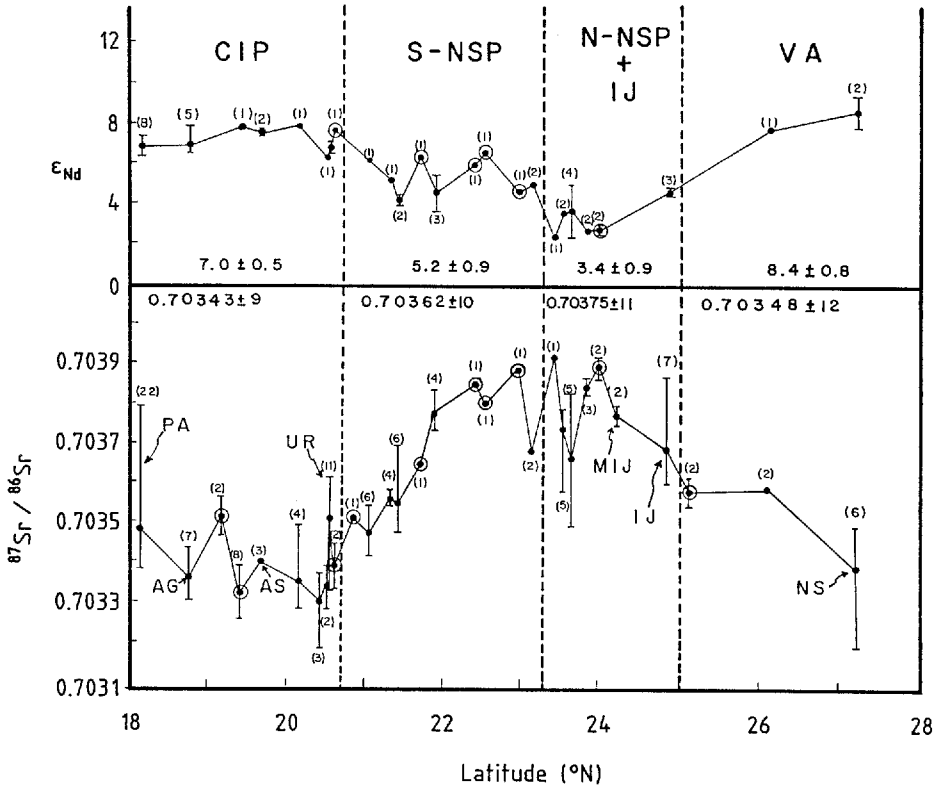

Fig. 3. The variation of Sr- and Nd-isotopic composition along the Mariana and Volcano arc. *Numbers in parentheses* indicate the number of analyses involved in determining the mean (*solid dot*) and range (*bars*) for each volcano. *Large circles* denote extinct edifices. Means ± 1 standard deviation are shown for the studied portions of the CIP, S-NSP, N-NSP through to Iwo Jima, and VA. Location of the major volcanic islands are also shown: *PA*, Pagan, *AG*, Agrigan, *AS*, Asuncion, *UR*, Uracas, *IJ*, Iwo Jima, *NS*, Nishino Shima. Additional $^{87}Sr/^{86}Sr$ and ε_{Nd} data for some volcanic islands are from various sources (DePaolo and Wasserburg 1977; Dixon and Batiza 1979; Stern 1981; Notsu et al. 1983; White and Patchett 1984; Woodhead and Fraser 1985; Ito and Stern 1986; Woodhead 1989)

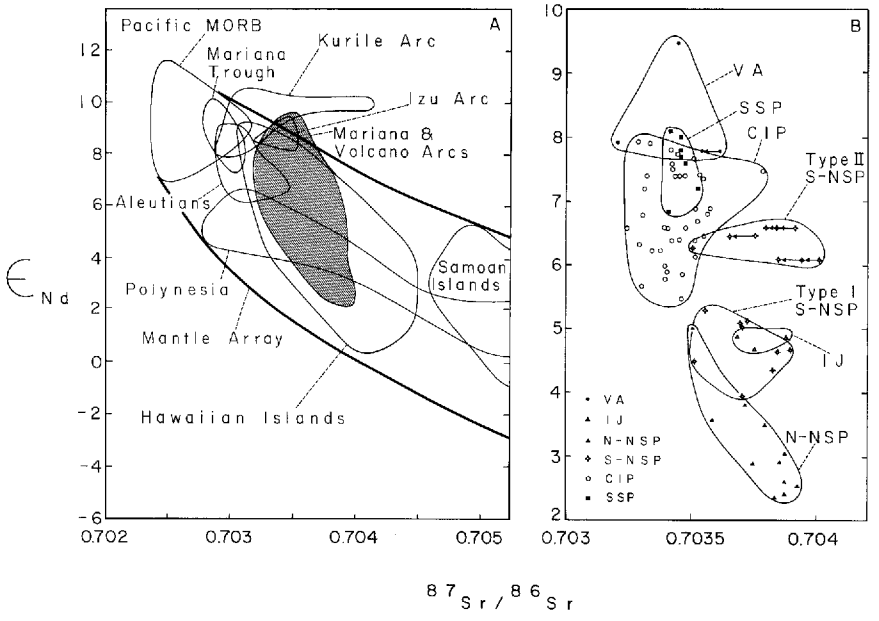

Fig. 4. Nd-Sr isotopic variation diagram. **A** The lavas of Mariana and Volcano arcs (*dark field*) are compared to OIB, MORB and other western Pacific arcs. The upper boundary of the Pacific mantle array (*bold line*) is defined by data from Pacific MORB (White and Hofmann 1982; Ito et al. 1987; White et al. 1987), Hawaiian islands (O'Nions et al. 1977; White and Hofmann 1982; Stille et al. 1983; Staudigel et al. 1984; Roden et al. 1984; Chen and Frey 1985) and Samoan islands (Wright and White 1986/87), whereas the lower boundary is defined by data for Polynesia (Vidal et al. 1984; Duncan et al. 1986) and Hawaiian islands. Also shown are fields for lavas from the Mariana Trough (Volpe et al. 1987), the Kurile arc (Zhuravelv et al. 1987), Aleutian arc (McCulloch and Perfit 1981; von Drach et al. 1986) and Izu arc (Nohda and Wasserburg 1981; Notsu et al. 1983). **B** Detailed $^{143}Nd/^{144}Nd$ vs $^{87}Sr/^{86}Sr$ variation diagram for the Mariana and Volcano arc segments. Leached and unleached samples are connected by *solid lines*. The *S-NSP* field is divided into type *I* and *II*, as discussed in the text. The *SSP* field is compiled from other sources (Dixon and Stern 1983; Stern and Bibee 1984). Additional data for the field of CIP are from DePaolo and Wasserburg (1977), Stern (1981), White and Patchett (1984), Dixon and Stern (1983) and Woodhead (1989)

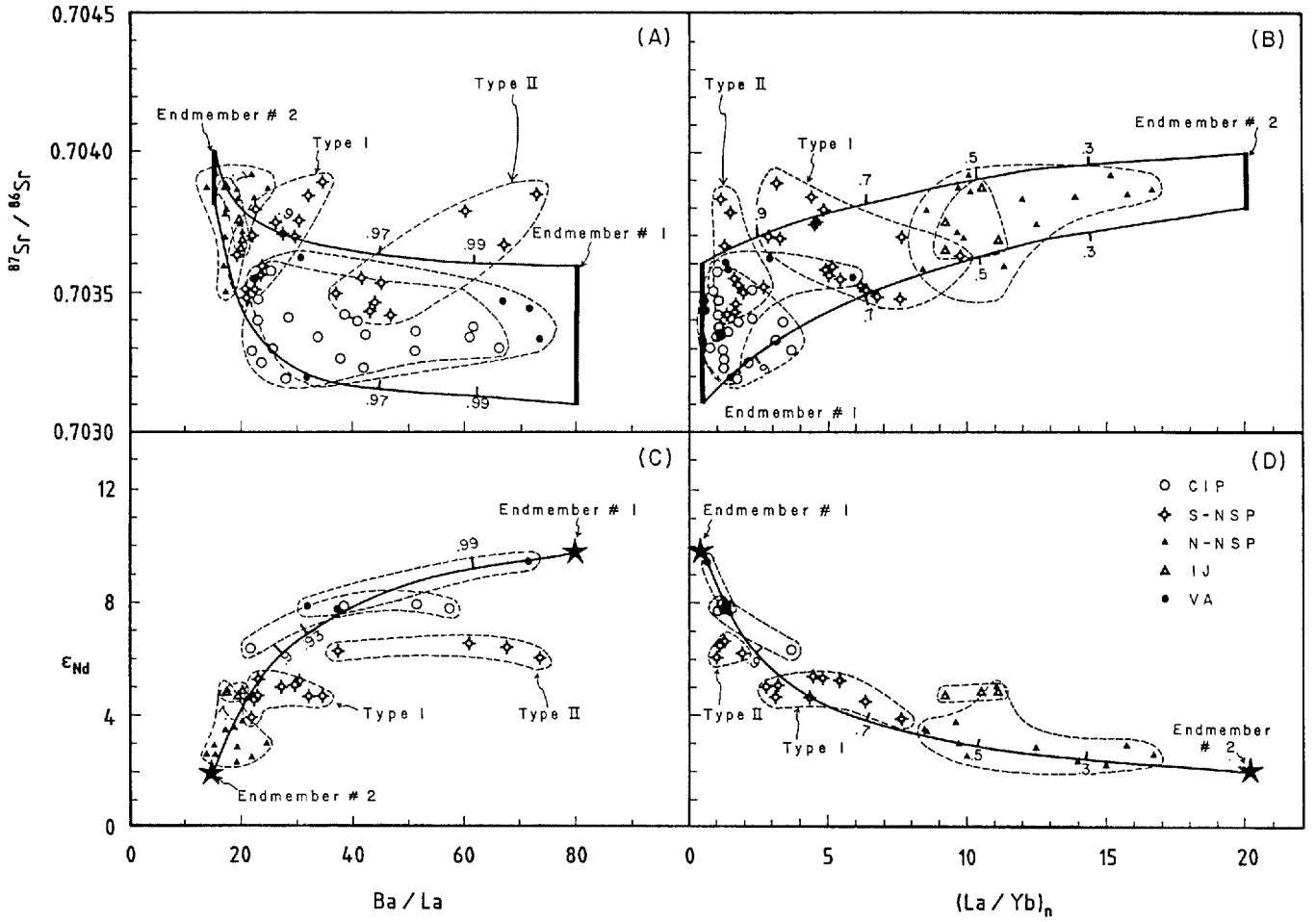

Fig. 5A–D. $^{87}Sr/^{86}Sr$ and ε_{Nd} vs Ba/La and $(La/Yb)_n$. The compositions of Endmembers #1 and #2 are from Table 2. The *solid lines* indicate mixing trajectories, with the *number* shown on the curve being the fraction of Endmember #1 involved in the mixture. Note that samples from the different arc segments fall into distinct fields as shown. Note that *S-NSP* lavas are subdivided into Type *I* and Type *II*. **A** $^{87}Sr/^{86}Sr$ vs Ba/La. **B** $^{87}Sr/^{86}Sr$ vs $(La/Yb)_n$. **C** ε_{Nd} vs Ba/La. **D** ε_{Nd} vs $(La/Yb)_n$

ples overlaps that of the CIP and the SSP, with $\varepsilon_{Nd} = +6.3$ to $+9.5$ and $^{87}Sr/^{86}Sr = 0.70319$ to 0.70357, whereas the N-NSP and Iwo Jima samples have radiogenic Sr and non-radiogenic Nd ($\varepsilon_{Nd} = +2.4$ to $+5.0$, $^{87}Sr/^{86}Sr = 0.70350$ to 0.70392) that fall well within the mantle array. Samples from the S-NSP lie between CIP and N-NSP and are displaced to higher $^{87}Sr/^{86}Sr$ at a given ε_{Nd}. For example, three extinct seamounts (Kasuga, D33-3-1; Fukuyama, D38-2; and Soyo, D41-52), contain higher $^{87}Sr/^{86}Sr$ (0.70375 to 0.70384) and thus extend the field of S-NSP lavas to the upper boundary of the mantle array. Lavas from the S-NSP form two distinct trends on a plot of Ba/La against $^{87}Sr/^{86}Sr$ (Fig. 5A). The existence of two distinct fields for S-NSP lavas leads us further to subdivide the S-NSP data into Type I (lower Ba/La at a given $^{87}Sr/^{86}Sr$) and Type II, as shown in Figs. 4 and 5.

Discussion

The Sr- and Nd-isotopic data presented here allow us to test a two-component mixing model (Fig. 2) for the evolution of the source region of the Mariana and Volcano arc system, previously proposed on the basis of LIL and REE data (Lin et al. 1989). The combination of the isotopic data with the trace element data shows that the results from the Mariana and Volcano arcs need three components to explain the entire range of geochemical variation. The test and the modification make up the first part of the following discussion, followed by a discussion of the significance of these results for our understanding of arc magma genesis.

Two component mixing model

The trace element characteristics of lavas from the Mariana and Volcano arcs have been interpreted to result from mixing of two distinct end-members (Lin et al. 1989). Endmember #1 is depleted mantle (or melt therefrom) similar to the source of MORB that has been metasomatized, while Endmember #2 (or melt therefrom) is LIL- and LREE-enriched OIB-like source. Based on the asymptotes of the mixing curves, Endmember #1 has $Ba/La \geq 70$ and $(La/Yb)_n \sim 0.5$, while

Table 2. Inferred trace element and isotope composition of End-members #1, #2, #3 and other data

Element (ppm)	End-member[a] #1	End-member[a] #2	PAWMS[b]	Endmember[c] #3 (Fluid)
Sr	470	1234	1144	217
Ba	150	1122	1338	400
La	1.87	74.8	25.8	3.8
Nd	5.9	48	19.3	2.1
Yb	2.5	2.5	5.55	0.6
ε_{Nd}	+9.7	+2	−3.3	−3.3
$^{87}Sr/^{86}Sr$	0.7031 0.7036	0.7038 0.7040	0.7083	0.7083
Ba/La	80	15	51.9	105
$(La/Yb)_n$	0.5	20	3.1	4.2
Sr/Nd	80	25.7	59	103

[a] Inferred from key element of Yb (=2.5 ppm) which is similar in Endmembers #1 and #2, and Ba/La=80, $(La/Yb)_n$=0.5 for Endmember #1, while Endmember #2 has Ba/La=15, $(La/Yb)_n$=20

[b] Pacific Authigenic Weighted Mean Sediment (PAWMS) from Hole et al. (1984). ε_{Nd} is from McCulloch and Wasserburg (1978) and $^{87}Sr/^{86}Sr$ from Stern and Ito (1983)

[c] Assuming the fluid is derived from PAWMS. Calculated using experimental data of the mobility of the element in the fluid (Tatsumi et al. 1986). The mobilities of Nd is from interpolation and assumed has 11%. ε_{Nd} from McCulloch and Wasserburg (1978), $^{87}Sr/^{86}Sr$ from Stern and Ito (1983)

Endmember #2 has Ba/La ~15 and $(La/Yb)_n \geq 18$. These end-members are shown in Fig. 5, where ε_{Nd} and $^{87}Sr/^{86}Sr$ are plotted against Ba/La and $(La/Yb)_n$. ε_{Nd} for both end-members is fairly well constrained by the asymptotes of the data arrays; ε_{Nd} of Endmember #1 is taken from the highest value observed for VA and is similar to Pacific MORB (ε_{Nd} = +9.7; Ito et al. 1987); a range of $^{87}Sr/^{86}Sr$ was taken from that observed for CIP and VA lavas (0.7031–0.7036). For Endmember #2, ε_{Nd} was chosen from the lowest value of N-NSP lavas (ε_{Nd} = +2) and a range of $^{87}Sr/^{86}Sr$ was inferred from data for NSP and IJ (0.7038–0.7040). These values are listed in Table 2, along with estimates of abundances for key elements. As Yb abundances are very similar along the arc (Lin et al. 1989), Ba and La abundances are calculated from constant Yb concentration and the inferred end-member ratios in Fig. 5.

Tests of the two-component mixing model were done by plotting the Sr- and Nd-isotopic data against Ba/La and $(La/Yb)_n$, the elemental ratios determined in the original model to be diagnostic of the end-members (Lin et al. 1989). The match between the data and that predicted from the model can be examined in Fig. 5A–D. Correspondences are generally good between the data and the calculated binary-mixing curves.

Closer examination of Fig. 5A–D indicates that some data points fall far from the curve, and define trends that are very different from those predicted by the two-component model. The problem is especially serious for lavas from the Mariana S-NSP which form two parallel trends in Fig. 5A that extend away from the mixing curve and towards another component that has high Ba/La and $^{87}Sr/^{86}Sr$. Some of the samples identified as Type II S-NSP may be altered, as demonstrated by the fact that $^{87}Sr/^{86}Sr$ could be lowered by leaching (D33-3-1; D38-2; D41-52). We do not think that the most significant part of the observed elevated Ba/La and $^{87}Sr/^{86}Sr$ only results from alteration, as this group of samples is also distinct on a plot of ε_{Nd} vs Ba/La (Fig. 5C) and in their Pb isotopic characteristics (Lin et al. 1988). Support for the inference that some S-NSP lavas reflect source histories that are not consistent with two-component mixing comes from consideration of the Nd-isotopic and Ba/La data. Several of the S-NSP data points extend well off of the mixing curves on plots of ε_{Nd} vs Ba/La (Fig. 5C), elements that should be negligibly affected except by extensive alteration. It is suggested that the fields defined by S-NSP Types I and II may reflect real variations in source compositions, though some samples reveal minor seawater alteration. These data force us to consider a more complex model for the origin of the Mariana-Volcano arc source heterogeneity, specifically to include a third component.

Three component mixing

To modify the model, it is necessary to infer some of the trace element and isotopic characteristics of the third component, and Ba/La is critical for this purpose. Elevated Ba/La ratios are characteristic for arc melts, and may result from a sedimentary component (Kay 1980; Perfit and Kay 1986). The conclusion that there may be an overwhelming sedimentary component in Endmember #3 is consistent with the observation that it must also have high $^{87}Sr/^{86}Sr$. Endmember #3 has almost no effect on the REE; two-component mixing is adequate to explain the co-variation of ε_{Nd} with $(La/Yb)_n$ (Fig. 5D). Endmember #3 is not observed to affect the REE budget. This indicates that the deviation of the S-NSP lavas from the two-component mixing array on the plot of $^{87}Sr/^{86}Sr$ vs $(La/Yb)_n$ is the result of addition of substantial amounts of radiogenic Sr, not LREE-depleted material (Fig. 5B). These considerations indicate that Endmember #3 has very high Sr/Nd and Sr isotopic composition, well above those seen in MORB or OIB.

It is difficult to argue that Endmember #3 is composed of bulk pelagic sediments. The values of Ba/La for Type II S-NSP lavas (37–74) are as high as, or higher than, those generally inferred for pelagic sediments. For example, Ba/La for sediments being subducted beneath the Aleutians is 52–69 (McCulloch and Perfit 1981), whereas the Pacific Authigenic Weighted Mean Sediment (PAWMS) has Ba/La of 52 (Hole et al. 1984). Furthermore, subducted pelagic sediments often have low Sr/Nd (Rogers et al. 1985; Ellam and Hawkesworth 1988). The average upper crust has 350 ppm Sr, 26 ppm Nd and Sr/Nd=13.5 (Taylor and McLennan 1985). However, the fluid derived from sediment may have high Ba/La and Sr/Nd since the mobility of Ba and Sr in hydrous fluid is much greater than that of La and Nd (Tatsumi et al. 1986). These observations support the argument that the high Ba/La and Sr/Nd of Endmember #3 is

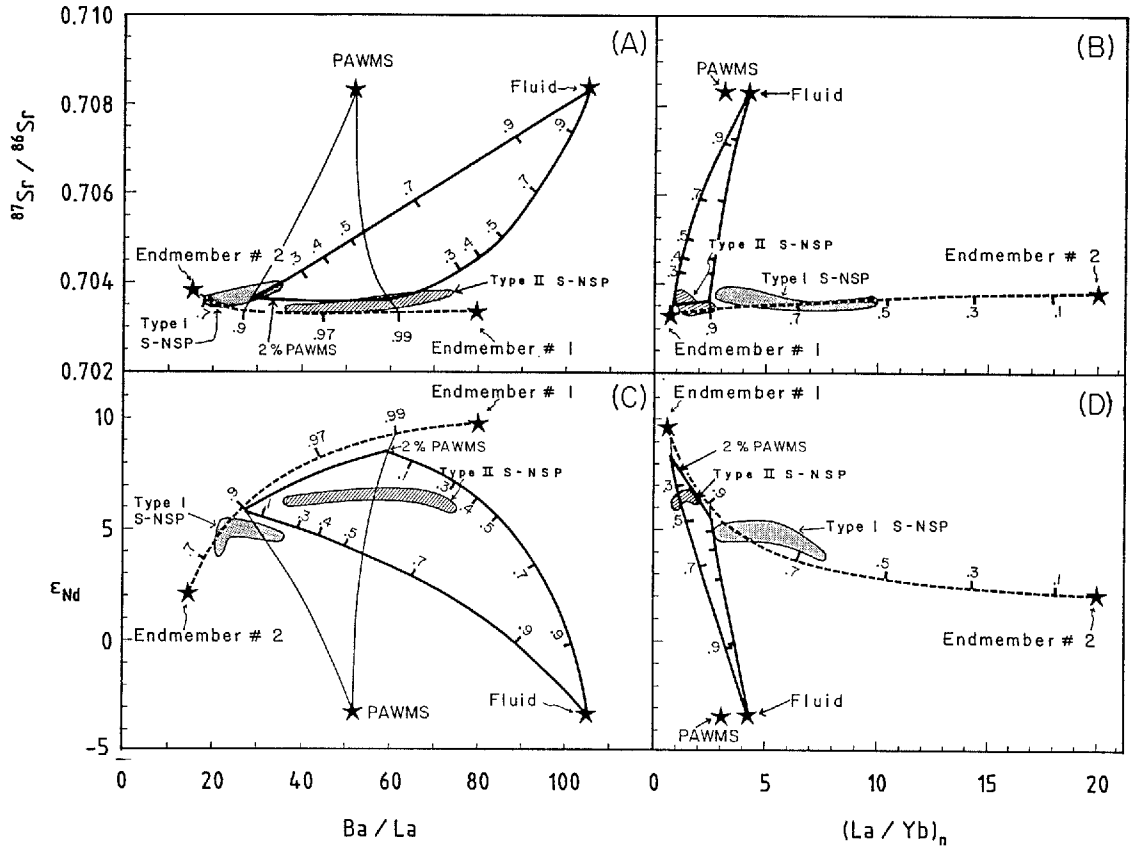

Fig. 6. Mixing model (Lin et al. 1989) by plotting of $^{87}Sr/^{86}Sr$ and ε_{Nd} vs Ba/La and $(La/Yb)_n$. The compositions of Endmembers #1 and #2 are from Table 2. The third component is represented by the fluid which was derived from Pacific Authigenic Weighted Mean Sediment (PAWMS) (Hole et al. 1984). The content of the trace element in the third component is calculated from various elemental mobility in the fluid of dehydration (Tatsumi et al. 1986) and assuming mobility of Nd is 11%. The *dashed line* indicate the mixing trajectories of Endmembers #1 and #2. The *thin solid line* is the curve for mixing of PAWMS and the hybrid of 99% Endmember #1 and 1% Endmember #2, and 90% Endmember #1 and 10% Endmember #2. The *contour* of 2% of PAWMS is also shown. The *bold solid line* is the curve for mixing of Endmember #3 with these sediment-contaminated hybrid sources. The number shown on the mixing curve indicates the fraction of Endmember #3 involved in the sediment-contaminated hybrid sources. The fields of Type *I* and Type *II S-NSP* are also shown for comparison. **A** $^{87}Sr/^{86}Sr$ vs Ba/La. **B** $^{87}Sr/^{86}Sr$ vs $(La/Yb)_n$. **C** ε_{Nd} vs Ba/La. **D** ε_{Nd} vs $(La/Yb)_n$

not derived from bulk sediments but rather from fluids derived from sediments.

The best explanation for the fact that S-NSP lavas have high to very high Ba/La, but other isotopic and trace element traits of mantle-derived rocks, is that Endmember #3 is a fluid with high concentrations of alkaline earths and low concentrations of REE. Recent experimental data indicate that the alkaline earths are much more soluble in high-P hydrous fluids than are the REE (Tatsumi et al. 1986). We therefore have modelled Endmember #3 as a hydrous fluid released as a result of dehydration of subducted sediments, assumed here to be PAWMS (Hole et al. 1984). These sediments are assumed to have $\varepsilon_{Nd} = -3.3$ (McCulloch and Wasserburg 1978) and $^{87}Sr/^{86}Sr = 0.7083$ (Stern and Ito 1983). The trace element contents of the sediment-derived fluid is calculated from PAWMS and according to experimental hydrous fluid/solid mobility factors (Tatsumi et al. 1986) (Table 2). We note that these experiments were conducted using serpentine, not sediments, as a starting material, but the general order of partitioning may hold during the dehydration of sediments as well. The model assumes that the cations from each gram of sediment are released into 1 gram of fluid derived from the sediment itself plus a much larger proportion from the dehydrating oceanic crust and mantle. The model assumes that the non-sedimentary portion of the subducted oceanic crust and mantle contributes no cations, only water.

It may be argued that the role of hydrous fluid derived from the altered subducted slab should also contribute some cations and water to the overlying mantle wedge. However, calculation of hydrous fluid derived from altered subducted slab (assumed altered MORB; Hole et al. 1984) using the elementary mobility data from Tatsumi et al. (1986) only can produce fluids with Ba/La = 17 and Sr/Nd = 17. These cannot be responsible for the high Ba/La and Sr/Nd of S-NSP lavas. Altered MORB may have higher $^{87}Sr/^{86}Sr$ (0.70334–0.70417; O'Nions and Pankhurst 1976) than fresh MORB (0.70232–0.70284; White et al. 1987). Nonetheless, ε_{Nd} of altered MORB is negligibly changed by seawater alteration. The low Ba/La, Sr/Nd and isotopic characteris-

tics of altered MORB, in fact, cannot explain the anomalous trend observed from S-NSP lavas as shown in Figs. 5A and 5C.

These arguments lead to fluid compositions listed as Endmember #3 in Table 2 and plotted in Fig. 6. Also plotted (Fig. 6A–D) are mixing trajectories between Endmember #3 and mixtures of 98% of hybrid of Endmembers #1 and #2 plus 2% of subducted sediment. The hybrid source is composed of 90–99% Endmember #1 and 1–10% Endmember #2. For the best fit between the model and the observed anomalous trend of S-NSP lavas, many different proportions of sediment were modelled. The result shows that 2% of sediment involvement best fits the trend defined by S-NSP lavas.

These are largely heuristic models, but demonstrate in a general way that a modification involving the addition of a third component containing high Ba and Sr, but negligible REE, is a substantial improvement over a model of two-component mixing.

Implications for the evolution of the source of Mariana and Volcano arc melts

The isotopic data presented here allow us to refine models for the evolution of the melt source region beneath the Mariana and Volcano arcs. The data generally substantiate a model of two-component mixing, involving an OIB-type mantle and a much more depleted MORB-like mantle that was metasomatically enriched prior to mixing. This model reconciles the arguments for a predominantly OIB-type mantle source for some arcs (Stern 1981; Morris and Hart 1983) with arguments for a predominantly metasomatized MORB-type mantle source (Perfit et al. 1980; Ellam and Hawkesworth 1988). Consideration of the isotopic data along with the trace element data allows the further identification of a third component, interpreted here as a metasomatic fluid (Endmember #3). Because mixing trajectories calculated for Endmember #3 extend back to the mixing array defined by Endmembers #1 and #2, we infer a temporal progression. Specifically, mixing between Endmembers #1 and #2 occurred *prior* to the influx of Endmember #3 which was restricted geographically as well as temporally. It must be recognized that Endmember #3 bears a very strong chemical resemblance to the metasomatic fluid that enriched MORB-like mantle in Ba and radiogenic Sr to generate Endmember #1, and that has been advocated for many arc systems (Perfit et al. 1980; Ewart and Hawkesworth 1987; Ellam and Hawkesworth 1988). However, the earlier metasomatism to form Endmember #1 predated what appears in the northernmost Marianas to be the more important mixing event, between Endmembers #1 and #2. Nevertheless, it is clear that fluids like Endmember #3 are, and have been, important controls on the composition of the Mariana and Volcano arc melt sources.

The spatial relationships and tectonic setting responsible for adding Sr- and Ba-enriched hydrous fluids to depleted MORB-like mantle, and to the mixtures of Endmembers #1 and #2, are obvious. The dehydrating subducted slab underlies the mantle sources. A hydrous fluid was expelled during dehydration of the slab, taking with it a substantial portion of the most soluble cations. Some of these (Sr, Ba) were already enriched in the sediments relative to the mantle and these should dominate the fluid composition. This low-density fluid rose into the overlying mantle wedge, where it enriched the mantle wedge in Sr and Ba and led to melting by depressing the solidus and encouraging diapiric upwelling (e.g., Plank and Langmuir 1988).

Why mixing between Endmembers #1 and #2 occurs is more difficult to understand. The observation that different segments of the arc are dominated by different proportions of each end-member is crucial: Endmember #1 dominates in the Mariana CIP and the Volcano arc north of Iwo Jima, probably as far north as Honshu (Nohda and Wasserburg 1981; Rubenstone et al. 1988). Endmember #2 dominates only in the portion of the arc adjacent to the northern end of the Mariana Trough back-arc basin, in the Mariana N-NSP and Iwo Jima.

Endmember #1 dominates the mature portions of the arc system. Arc volcanism in the Mariana CIP has not been interrupted since opening of the Mariana Trough, about 5 Ma (Hussong and Uyeda 1981), while the Volcano-Bonin-Izu arc system to the north has not been disturbed by rifting since the Parece Vela-Shikoku Basin opened in the Oligocene (Rodolfo 1980). We infer from this that magma generation beneath mature intra-oceanic arcs involves the production of low-K arc tholeiites and high alumina basalt melts that tap mantle sources similar to that of Endmember #1. This conclusion is supported by consideration of global data bases (Perfit et al. 1980; Plank and Langmuir 1988), in addition to being consistent with the regional geology.

The observation that shoshonitic lavas (melts dominated by Endmember #2) are restricted to the part of the arc adjacent to the northern termination of the Mariana Trough supports the argument that the back-arc basin rift is propagating northward. Shoshonitic lavas erupt first during the re-initiation of a new arc following back-arc rifting. This is argued to be a consequence of the diapiric upwelling of deeper, more fertile parts of the mantle, either in response to, or as a harbinger of, rift initiation (Stern et al. 1988). Displacing such mantle up to the top of the sub-arc asthenosphere where melting occurs (Lin et al. 1989) results in the generation of shoshonitic lavas. The enriched source becomes progressively more depleted of its inventory of incompatible elements as the new arc segment ages. With only a variable recharge of LIL elements from the dehydrating slab, the sub-arc mantle soon becomes capable of generating only arc tholeiites and low-K, high-alumina basalt.

The model that shoshonitic magmatism in the Mariana N-SNP and Iwo Jima is the consequence of rift propagation is by no means proved. Alternatively, there may be some sort of a fixed 'hot-spot' in the region causing fertile mantle to be injected into the sub-arc zone of melting. Inspection of the isotopic variations along the arc indicates a more symmetrical distribution centered on the Mariana N-NSP and Iwo Jima (Fig. 3) than

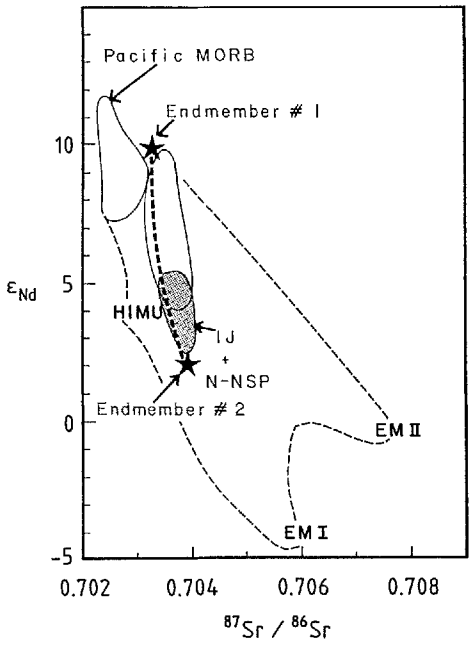

Fig. 7. Plot of ε_{Nd} vs $^{87}Sr/^{86}Sr$ for Mariana and Volcano arc lavas showing the fields occupied by plausible mantle components. The *trajectory* defined by the 2-component mixing model is also shown here for comparison. The *shaded field* is defined by lavas from *IJ* and *N-NSP* while the *solid field* is defined by *SSP*, *CIP*, *S-NSP* and *VA*. Data sources of Pacific MORB are similar to Fig. 3. Mantle components HIMU, EMI and EMII are from Hart (1988). The trend of IJ and N-NSP comes close to HIMU and extends toward EMI, suggesting that the OIB source for IJ and N-NSP melts may have HIMU and EMI type mantle components. Note that the trend towards Endmember #2 does not extend toward EMII, interpreted to represent subducted and recycled continental material (Hart 1988). Note also that Endmember #1 is displaced to the high $^{87}Sr/^{86}Sr$ side of MORB, indicating that radiogenic Sr has been added to the depleted mantle

observed for the trace elements (Lin et al. 1989), an observation that favors a hot-spot interpretation.

In addition, a plot of ε_{Nd} versus $^{87}Sr/^{86}Sr$ (Fig. 7) indicates that the field of IJ and N-NSP is close to HIMU (high U/Pb mantle component; Hart 1988) and extends toward EMI (type I enriched mantle components; Hart 1988), similar to the trend of Hawaiian islands. Nonetheless, Sr-Pb and Nd-Pb isotopic systematics (J.D. Morris, unpublished data) indicate IJ lavas have characteristics transitional to HIMU while N-NSP lavas extend toward EMII (Type II enriched mantle components) instead of EMI. Resolution of this problem must await more lead isotopic data. Whatever the enriched mantle is, however, the Sr-Nd isotopic data support the argument that an OIB-like mantle is involved in the source region of IJ and N-NSP magma.

Whatever tectonic model is applied, two conclusions are plausible. First, the isotopic and trace element data require a mantle source for the enrichments, and so preclude interpretations that the subducted slab is the source of Endmember #2. Second, whatever the ultimate source of the fertile mantle, immediately prior to diapirism it must be located above the subducted slab, within the upper 150 km of the mantle.

In either propagating-rift or fixed hot-spot model, Endmembers #1 and #2 can be expected to mix during the diapiric upwelling of fertile mantle (Endmember #2) to partially displace depleted mantle (Endmember #1). The scale of hybridization is unknown, but the mixing trajectories are readily interpreted as resulting from the preferential melting of Endmember #2 domains, with an increasing proportion of Endmember #1 involved in the melt as the fertile mantle is exhausted. A 'plum-pudding' model of Endmember #2 'plums' in an Endmember #1 'pudding' may be the ultimate result, consistent with studies of Fiji (Gill 1984) and the Aleutians (Morris and Hart 1983). If water contents were similar between 'plums' and 'pudding', melting should first and most extensively involve the fertile mantle (Endmember #2). After Endmember #2 was exhausted, Endmember #1 would be melted. Endmember #3 would be added continuously to the mantle wedge, but may not be identifiable until Endmember #2 had been largely removed from the mixture. Note that in Fig. 6, Endmember #3 is identified where it has been added to mixtures of about 90–99% Endmember #1. From this point until no more Endmember #2 may be identified in the mixture, the effect of Endmember #3 is to reinforce the metasomatically induced characteristics of Endmember #1.

Conclusions

The characteristics of the LIL and REE of the lavas from the Mariana and Volcano arcs demonstrate that two different sources were mixed and tapped. One is a variably metasomatized depleted mantle or melt (Endmember #1) and the other is a LIL- and LREE-enriched OIB-like source or melt (Endmember #2). The isotopic characteristics of Mariana and Volcano arcs lavas support this interpretation. The samples fall in the field of ocean-island basalt and extend along the mantle array. Sr- and Nd-isotopic compositions exhibit variation along the arc. High $^{87}Sr/^{86}Sr$ (0.70350–0.70392) and low ε_{Nd} (+2.6 to +5.1) were found in the N-NSP and Iwo Jima supporting the inference that magmas from this part of the arc are dominated by an OIB-like mantle source. The relatively lower $^{87}Sr/^{86}Sr$ (0.70320–0.70362) and higher ε_{Nd} (+6.4 to +9.6) found for the VA and the CIP are consistent with the observation that this part of the arc erupts lavas which are derived from metasomatized depleted mantle. Constraints imposed by the isotopic and trace element data require a mantle source enriched by fluids from the subducted slab. Samples from S-NSP have higher $^{87}Sr/^{86}Sr$ at a given ε_{Nd}, as well as Ba/La exceeding that of Pacific sediment. A minor decrease in $^{87}Sr/^{86}Sr$ of leached S-NSP lavas between 2.5N and 6N HCl treatment indicates cryptic alteration of these lavas that even the 6N HCl treatment may not have removed. However, anomalous trends on the plots of Sr- and Nd-isotopic compositions versus incompatible trace element ratios indicate that a third component may exist. A plausible candidate for this component is a minor amount of subducted sediment and low proportion of metasomatic fluid derived from sediment. The general agreement of the three-component mixing model with the data indicates that most Mariana and Volcano arc melts result from the mixture of varia-

bly metasomatized depleted mantle or melt (Endmember #1) and a LIL-, LREE-enriched, OIB-like source or melt (Endmember #2). On the other hand some Mariana S-NSP melts are generated from hybrids of Endmembers #1 and #2 that are contaminated by minor amounts of sediment and sediment-derived fluid (Endmember #3). It is inferred that fertile mantle (Endmember #2) was progressively exhausted since the hybrids were generated, so that depleted mantle (Endmember #1) comes to dominate melt compositions during the evolution of the arc. The influx of sediment-derived fluid (Endmember #3) occurred after mixing of Endmembers #1 and #2.

Acknowledgements. We would like to thank the Department of Terrestrial Magnetism of the Carnegie Institution of Washington for the use of their mass-spectrometer to measure Nd isotope. We are grateful to S.B. Shirey and R.W. Carlson for their enthusiastic assistance during the analyses. We thank the officers and crew of the R/V Thomas Thompson for assistance in sample collection. The manuscript was greatly improved by comments from RW Kay, JD Myers and other anonymous reviewers. This work was supported by NSF grants OCE-8415699 and OCE-8415739. This is University of Texas at Dallas Programs in Geosciences Contribution no. 652.

References

Arculus RJ, Johnson RW (1978) Criticism of generalized models for the magmatic evolution of arc-trench systems. Earth Planet Sci Lett 39:118–126

Arculus RJ, Powell R (1986) Source component mixing in the region of arc magma generation. J Geophys Res 91:5913–5926

Armstrong RL (1971) Isotopic and chemical constraints on models of magma genesis in volcanic arcs. Earth Planet Sci Lett 12:137–142

Batiza R (1984) Inverse relationship between Sr isotope diversity and rate of oceanic volcanism has implications for mantle heterogeneity. Nature 309:440–441

Bloomer SH, Stern RJ, Smooth NC (1989a) Physical volcanology of the submarine Mariana and Volcano Arcs. Bull Volcanol 51:210–224

Bloomer SH, Stern RJ, Fisk E, Geschwind CH (1989b) Shoshonitic volcanism in the northern Mariana Arc: 1, Mineralogic and major and trace element characteristics. J Geophys Res 94:4469–4496

Chase TE, Menard HW, Mammerickx J (1968) Bathymetry of the North Pacific (Chart no. 6). Institute of Marine Resources, Technical Report Series TR-11

Chen CY, Frey FA (1985) Trace element and isotopic geochemistry of lavas from Haleakala Volcano, East Maui, Hawaii: implications for the origin of Hawaiian basalts. J Geophys Res 90:8743–8768

Chow TJ, Stern RJ, Dixon TH (1980) Absolute and relative abundances of K, Rb, Sr, and Ba in circum-Pacific island-arc magmas, with special reference to the Marianas. Chem Geol 28:111–121

Davies GF (1984) Geophysical and isotopic constraints on mantle convection: an interim synthesis. J Geophys Res 89:6017–6040

DePaolo DJ, Wasserburg GJ (1977) The sources of island arcs as indicated by Nd and Sr isotopic studies. Geophys Res Lett 4:465–468

Dixon TH, Batiza R (1979) Petrology and chemistry of recent lavas in the Northern Marianas: implications for the origin of island arc basalts. Contrib Mineral Petrol 70:167–181

Dixon TH, Stern RJ (1983) Petrology, chemistry and isotopic composition of submarine volcanoes in the southern Mariana arc. Geol Soc Am Bull 94:1159–1172

Dixon TH, Batiza R, Futa K, Martin D (1984) Petrochemistry, age, and isotopic composition of alkali basalts from Ponape Island, western Pacific. Chem Geol 43:1–28

von Drach V, Marsh BD, Wasserburg GJ (1986) Nd and Sr isotopes in the Aleutians: multicomponent parenthood of island-arc magmas. Contrib Mineral Petrol 92:13–34

Duncan RA, McCulloch MT, Barsczus HG, Nelson DR (1986) Plume versus lithospheric sources for melts at Ua Pou, Marquesas Islands. Nature 322:534–538

Ellam RM, Hawkesworth CJ (1988) Elemental and isotopic variation in subduction related basalts: Evidence for a three component model. Contrib Mineral Petrol 98:72–80

Ewart A, Hawkesworth CJ (1987) The Pleistocene-Recent Tonga-Kermadec Arc lavas: Interpretation of new isotopic and rare earth data in terms of a depleted mantle source model. J Petrol 28:495–530

Garcia MO, Liu NWK, Muenow DW (1979) Volatiles in submarine volcanic rocks from the Mariana Island arc and trough. Geochim Cosmochim Acta 43:305–312

Gill JB (1984) Sr-Pb-Nd isotopic evidence that both MORB and OIB sources contribute to oceanic island arc magmas in Fiji. Earth Planet Sci Lett 68:443–458

Hart SR (1988) Heterogeneous mantle domains: signatures, genesis and mixing chronologies. Earth Planet Sci Lett 90:273–296

Hole MJ, Saunders AD, Marriner GF, Tarney J (1984) Subduction of pelagic sediments: implications for the origin of Ce-anomalous basalts from the Mariana Islands. J Geol Soc London 141:453–472

Honza E, Tamaki K (1985) The Bonin Arc. In: Nairn A, Stehli H, Uyeda S (eds) The Ocean Basins and Margins, vol 7A, Plenum Press, NY, pp 459–502

Hussong DM, Uyeda S (1981) Tectonic processes and the history of the Mariana arc: a synthesis of the results of Deep Sea Drilling Project Leg 60. In: Hussong DM, Uyeda et al. (eds) Initial Report DSDP 60, US Printing Office, Washington, pp 909–929

Ito E, Stern RJ (1986) Oxygen- and strontium-isotopic investigations of subduction zone volcanism: the case of the Volcano Arc and the Mariana Island Arc. Earth Planet Sci Lett 76:312–320

Ito E, White WM, Gopel C (1987) The O, Sr, Nd and Pb isotope geochemistry of MORB. Chem Geol 62:157–176

Jackson MC, Fryer P (1988) Chemical evolution of shoshonitic lavas at the Kasuga submarine volcanoes, northern Mariana arc. EOS 69:1470

Kay RW (1980) Volcanic arc magmas: Implications for a melting-mixing model for element recycling in the crust-upper mantle system. J Geol 88:497–522

Lin PN, Stern RJ, Bloomer SH, Morris J (1986) Alkalic submarine volcanism in the Northern Mariana and Southern Izu Arc: REE and radiogenic isotope data. EOS 67:1277

Lin PN, Stern RJ, Morris J, Ito E, Bloomer SH (1988) Constraints on melt sources for the northern Mariana and southern Volcano arcs: LIL, REE, Sr-, Nd-, Pb-, and O-isotopic evidence. EOS 69:505

Lin PN, Stern RJ, Bloomer SH (1989) Shoshonitic volcanism in the northern Mariana arc, 2. Large-ion lithophile and rare earth element abundances: evidence for the source of incompatible element enrichments in intraoceanic arcs. J Geophys Res 94:4497–4514

McCulloch MT, Wasserburg GJ (1978) Sm-Nd and Rb-Sr chronology of continental crust formation. Science 200:1003–1011

McCulloch MT, Perfit MR (1981) $^{143}Nd/^{144}Nd$, $^{87}Sr/^{86}Sr$ and trace element constraints on the petrogenesis of Aleutian island arc magmas. Earth Planet Sci Lett 56:167–179

McLennan SM, Taylor SR (1981) Role of subducted sediment in island-arc magmatism: constraints from REE pattern. Earth Planet Sci Lett 54:424–430

Meijer A (1976) Pb and Sr isotopic data bearing on the origin of volcanic rocks from the Mariana island-arc system. Geol Soc Am Bull 87:1358–1369

Meijer A, Reagan M (1981) Petrology and geochemistry of the island of Sarigan in the Mariana Arc: calc-alkaline volcanism in an oceanic setting. Contrib Mineral Petrol 77:337–354

Morris JD, Hart SR (1983) Isotopic and incompatible element constraints on the genesis of island arc volcanics from Cold Bay and Amak Island, Aleutians, and implications for mantle structure. Geochim Cosmochim Acta 47:2015–2030

Nier AO (1950) A redetermination of the relative abundances of the isotopes of carbon, nitrogen, oxygen, argon, and potassium. Phys Rev 77:789–793

Nohda S, Wasserburg GJ (1981) Nd and Sr isotopic study of volcanic rocks from Japan. Earth Planet Sci Lett 52:264–276

Notsu K, Isshiki N, Hirano M (1983) Comprehensive strontium isotope study of Quaternary volcanic rocks from the Izu-Ogasawara arc. Geochem J 17:289–302

O'Nions RD, Pankhurst RJ (1976) Sr isotope and rare earth element geochemistry of DSDP Leg 37 basalts. Earth Planet Sci Lett 31:255–261

O'Nions RK, Hamilton PJ, Evensen NM (1977) Variations in $^{143}Nd/^{144}Nd$ and $^{87}Sr/^{86}Sr$ ratios in oceanic basalts. Earth Planet Sci Lett 34:13–22

Perfit MR, Kay RW (1986) Comment on "Isotopic and incompatible element constraints on the genesis of island arc volcanics from Cold Bay and Amals Island, Aleutians, and implications for mantle structure" by Morris JD and Hart SR. Geochim Cosmochim Acta 50:477–481

Perfit MR, Gust DA, Bence AE, Arculus RJ, Taylor SR (1980) Chemical characteristics of island-arc basalts: implications for mantle sources. Chem Geol 30:227–256

Plank T, Langmuir CH (1988) An evaluation of the global variations in the major element chemistry of arc basalts. Earth Planet Sci Lett 90:349–370

Richard P, Shimizu N, Allegre CJ (1976) $^{143}Nd/^{146}Nd$, a natural tracer: An application to oceanic basalts. Earth Planet Sci Lett 31:269–278

Roden MF, Frey FA, Clague DA (1984) Geochemistry of tholeiitic and alkalic lavas from the Koolau Range, Oahu, Hawaii: implications for Hawaiian volcanism. Earth Planet Sci Lett 69:141–158

Rodolfo KS (1980) Sedimentological summary: Clues to arc volcanism, arc sundering, and back-arc spreading in the sedimentary sequences of Deep Sea Drilling Project Leg 59. In: Kroenke L, Scott R et al. (eds) Initial Reports DSDP 59, US Printing Office, Washington, pp 621–623

Rogers NW, Hawkesworth CJ, Parker RJ, Marsh JR (1985) The geochemistry of potassic lavas from Vulsini, central Italy and implications for mantle enrichment processes beneath the Roman region. Contrib Mineral Petrol 90:244–257

Rubenstone JL, Zhang Y, Langmuir CH (1988) Geochemistry of the Izu Arc and Rift: constraints on spatial heterogeneity in the sub-arc mantle. EOS 69:1471

Staudigel H, Zindler A, Hart SR, Leslie T, Chen CY, Clague D (1984) The isotope systematics of a juvenile intraplate volcano: Pb, Nd, and Sr isotope ratios of basalts from Loihi Seamount, Hawaii. Earth Planet Sci Lett 69:13–29

Stern RJ (1979) On the origin of andesite in the northern Mariana Island arc: implications from Agrigan. Contrib Mineral Petrol 68:207–219

Stern RJ (1981) A common mantle source for western Pacific island arc and "hot-spot" magma – implications for layering in the upper mantle. Carnegie Inst Washington Yearb 80:455–462

Stern RJ (1982) Strontium isotopes from circum-Pacific intra-oceanic island arcs and marginal basin: regional variations and implication for magmagenesis. Geol Soc Am Bull 93:477–486

Stern RJ, Ito E (1983) Trace-element and isotopic constraints on the source of magmas in the active Volcano and Mariana Island Arcs, western Pacific. J Volcanol Geotherm Res 18:461–482

Stern RJ, Bibee LD (1984) Esmeralda Bank: geochemistry of an active submarine volcano in the Mariana Island Arc. Contrib Mineral Petrol 86:159–169

Stern RJ, Bloomer SH, Lin PN, Ito E, Morris J (1988) Shoshonitic magmas in nascent arcs: New evidence from submarine volcanoes in the northern Marianas. Geology 16:426–430

Stern RJ, Lin PN, Morris J, Jackson MC, Fryer P, Bloomer SH, Ito E (1990) Enriched Back-Arc Basin Basalts from the Northern Mariana Trough: Implications for the Magmatic Evolution of Back-Arc Basins. Earth Planet Sci Lett, in press

Stille P, Unruh DM, Tatsumoto M (1983) Pb, Sr, Nd and Hf isotopic evidence of multiple sources for Oahu, Hawaii basalts. Nature 304:25–29

Tatsumi Y, Hamilton DL, Nesbitt RW (1986) Chemical characteristics of fluid phase released from a subducted lithosphere and origin of arc magmas: Evidence from high-pressure experiments and natural rocks. J Volcanol Geotherm Res 29:293–309

Taylor SR, McLennan SM (1985) The continental crust: its composition and evolution. Blackwell Scientific Publications, 312 p

Vargas RH, Reagan MK (1987) Temporal variation of isotope and rare earth element abundances in volcanic rocks from Guam: implications for the evolution of the Mariana Arc. Contrib Mineral Petrol 97:497–508

Vidal P, Chauvel C, Brousse R (1984) Large mantle heterogeneity beneath French Polynesia. Nature 307:536–538

Volpe AM, Macdougall JD, Hawkins JW (1987) Mariana Trough basalts (MTB): trace element and Sr-Nd isotopic evidence for mixing between MORB-like and Arc-like melts. Earth Planet Sci Lett 82:241–254

Walker RJ, Carlson RW, Shirey SB, Boyd FR (1989) Os, Sr, Nd and Pb isotope systematics of southern African Peridotite xenoliths: Implications for the chemical evolution of subcontinental mantle. Geochim Cosmochim Acta 53:1583–1595

White WM, Hofmann AW (1982) Sr and Nd isotope geochemistry of oceanic basalts and mantle evolution. Nature 296:821–825

White WM, Patchett J (1984) Hf-Nd-Sr isotopes and incompatible element abundances in island arcs: implications for magma origins and crust-mantle evolution. Earth Planet Sci Lett 67:167–185

White WM, Dupre B (1986) Sediment subduction and magma genesis in the Lesser Antilles: isotopic and trace element constraints. J Geophys Res 91:5927–5941

White WM, Hofmann AW, Puchelt H (1987) Isotope geochemistry of Pacific Mid-Ocean Ridge Basalt. J Geophys Res 92:4881–4893

Wood DA, Marsh NG, Tarney J, Joron JL, Fryer P, Treuil M (1981) Geochemistry of igneous rocks recovered from a transect across the Mariana Trough, Arc, Fore-Arc, and Trench, sites 453 through 461, Deep Sea Drilling Project Leg 60. In: Hussong DM, Uyeda S et al. (eds) Init Repts DSDP 60, US Printing Office, Washington, pp 611–645

Woodhead JD, Fraser DG (1985) Pb, Sr and ^{10}Be isotopic studies of volcanic rocks from the Northern Mariana Islands, implications for magma genesis and crustal recycling in the Western Pacific. Geochim Cosmochim Acta 49:1925–1930

Woodhead JD, Harmon RS, Fraser DG (1987) O, S, Sr, and Pb isotope variations in volcanic rocks from the Northern Mariana Islands: implications for crustal recycling in intra-oceanic arcs. Earth Planet Sci Lett 83:39–52

Woodhead JD (1988) The origin of geochemical variations in Mariana lavas: A general model for petrogenesis in intra-oceanic island arcs? J Petrol 29:805–830

Woodhead JD (1989) Geochemistry of the Mariana arc (western Pacific): source composition and processes. Chem Geol 76:1–24

Wright E, White WM (1986/87) The origin of Samoa: new evidence from Sr, Nd, and Pb isotopes. Earth Planet Sci Lett 81:151–162

Zhuravlev DZ, Tsvetkov AA, Zhuravlev AZ, Gladkov NG, Chernyshev IV (1987) $^{143}Nd/^{144}Nd$ and $^{87}Sr/^{86}Sr$ ratios in recent magmatic rocks of the Kurile Island arc. Chem Geol (Isotope Geoscience Section) 66:227–243

Zindler A, Staudigel H, Batiza R (1984) Isotope and trace element geochemistry of young Pacific seamounts: implications for the scale of upper mantle heterogeneity. Earth Planet Sci Lett 70:175–195

Editorial responsibility: J. Patchett